The effect of native Al$_2$O$_3$ skin disruption on properties of fine Al powder compacts

Martin Balog [a,*], Cecilia Poletti [b], Frantisek Simancik [a], Martin Walcher [c], Walter Rajner [c]

[a] Institute of Materials and Machine Mechanics, Slovak Academy of Sciences, Racianska 75, 83102 Bratislava, Slovakia
[b] Institute of Materials Science and Technology, Vienna University of Technology, Karlsplatz 13/E308, A1040 Vienna, Austria
[c] NMD - New Materials Development GmbH., St. Pantaleon, Austria

ARTICLE INFO

ABSTRACT

In the presented study we characterize how various powder metallurgical routes (extrusion, forging, and HIP/sintering) affect the fracture of native Al$_2$O$_3$ layer present on the surface of ultra-fine atomized Al powders. It is shown that the different distribution, morphology and interconnectivity of in situ introduced Al$_2$O$_3$ dispersoids strongly affect the thermal stability and mechanical and thermal properties of subsequent powder compacts.

© 2010 Elsevier B.V. All rights reserved.

1. Introduction

In the field of powder metallurgy (PM) the use of ultra-fine Al powders brings up new appealing benefits when compared to coarse powders. Compacts of ultra fine Al powders are generally included to the group of materials known as SAP material. SAP, which denotes "Sinter-Aluminium-Pulver" (sintered aluminium powder), is a dispersion-strengthened Al–Al$_2$O$_3$ composite prepared via different powder metallurgical approaches [1]. SAP materials offer superior mechanical properties, creep behaviour and structural stability at elevated temperatures even after prolonged high temperature exposures [1–3]. These properties are in distinct contrast with all conventional Al alloys. SAP gained considerable attention in the middle of last century [1,4,5]. Better availability of fine atomized Al powders and more established Al powder metallurgy in hand with new characterization techniques led recently to new ideas employing fine atomized Al powders [6,7].

The properties of ultra-fine atomized powder compacts stem from the extraordinary stabilization and strengthening effects of in situ introduced nano-metric Al$_2$O$_3$ dispersoids [6]. In situ Al$_2$O$_3$ dispersoids originate and form from ∼3 nm thick native oxide skin [8,9] present on as-atomized Al powder particles. Nano-metric dispersoids do not tend to act as micro-concentrators, are not susceptible to cleavage and do not cause formation of voids. As a result,

superior mechanical properties can be attained at substantially lower dispersion contents when compared to micro-metric dispersoids [10]. Depending on processing route, native oxide skin layer either disrupts into separate nano-metric dispersoids or remains as continuous interpenetrating layer within final compacts [11]. Amount, morphology and distribution of nano-metric oxide dispersoids are expected to significantly affect the properties of compacts.

The objective of the presented work is to characterize how the fracture of native oxide skin during consolidation affects the properties of the powder compacts. Air atomized Al 99.8% powder with large surface area was used for this study. Three consolidation routes (direct extrusion, forging and hot isostatic pressing) were used in order to prepare representative types of the compacts with different extents of oxide skin disruption.

2. Experimental

Air atomized Al powder of technical purity (99.8%) was supplied by the company *New materials development G.m.bH.* [12]. Nominal diameters $d_{10} = 0.66\,\mu$m, $d_{50} = 1.31\,\mu$m, and $d_{90} = 2.51\,\mu$m were determined by Sympatec HELOS laser diffraction method. Al powder featured irregular morphology with abundant fine powder particles detached on the surface. Each powder particle represents a single monocrystal. The powder surface area $4.54\,\mathrm{m^2/g}$ was determined by using BET method. BET diameter was calculated according $d_{BET} = 6/(BET \cdot \rho_{Al})$, where ρ_{Al} is the density of Al. Due to irregular morphology of powder rather small $d_{BET} = 0.48\,\mu$m was obtained. Calculated Al$_2$O$_3$ content on as-atomized Al powder, using an average oxide thickness of 3 nm, was found to be 3.6 vol.%. 1.6 wt.% oxygen content on loose powders was determined by hot gas extraction (Ströhlein). Detailed description of the powder can be found in [6,13,14].

Loose powder was cold isostatically pressed (CIP) at 200 MPa with vacuum assistance prior consolidation. As proved by mercury porosimetry, CIP performs

* Corresponding author. Tel.: +421 259309414; fax: +421 244253301.
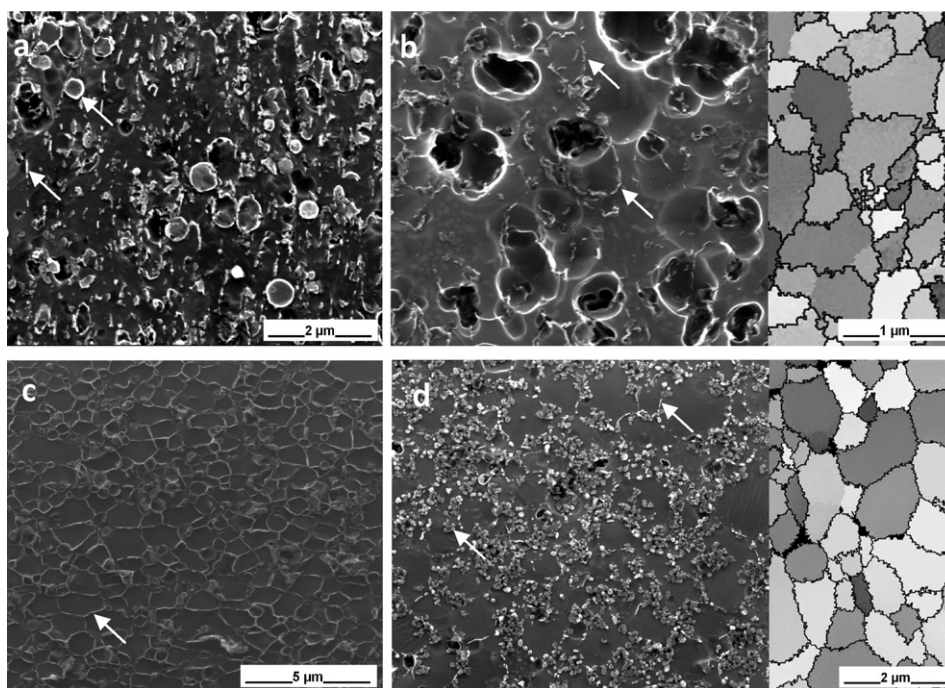E-mail address: ummsbama@savba.sk (M. Balog).

Fig. 1. SE SEM images of fine Al powder compacts prepared via direct extrusion in longitudinal (a) and transversal (b) direction, via forging (c) and via HIP (d). Corresponding EBSD maps are shown for directly extruded (transversal direction) and HIP compacts. The arrows indicate the alumina phase.

exhibited uniform pores distribution with ~78% of all pores found within 32–60 nm size and median pore radius 38 nm. Archimedes's density and mercury porosimetry measurements confirmed relative densities of CIP powder preforms to be 89% of theoretical density. CIP preforms were compacted by direct extrusion (DE), forging (F) or hot isostatic pressing (HIP). DE was performed at an extrusion temperature of 450 °C, average ram speed ~1 mm s^{-1} using extrusion ratio R = 11:1. Extrusion pressure monitored during DE consolidation reached a breakthrough value of 986 MPa. F was performed using a spindle press at 450 °C, 90 kJ of press energy and a maximal speed of 550 mm s^{-1}. No powder surface treatment was done prior DE and F. Vacuum degassing of canned CIP preforms at 350 °C for 24 h was performed prior HIP. Once sufficiently low vacuum (~10 Pa) was reached, HIP at 500 °C under 100 MPa pressure for 2 h dwell was performed. Alternatively to HIP, vacuum sintering of CIP preforms within temperature range 450–550 °C for 12 h dwell time and 10^{-3} Pa vacuum pressure was carried out as well.

In order to study the thermal stability of compacted materials air annealing at temperatures of 450 °C for 336 h, 500 °C for 24 h and 520 °C for 24 h was applied.

Samples were examined using FEG-SEM FEI Quanta 200 and TEM Jeol JEM 200CX. Samples were etched prior SEM observations. Electron Back Scatter Diffraction (EBSD) was used to measure the crystallographic grain orientations and to determine the grain size distribution. To clearly demonstrate the presence and distribution of nano-scale oxide dispersoids samples for TEM observation were prepared by electroetching followed by ion polishing applied for short time. Such treated samples featured oxide dispersoids that tilted and protruded over the etched Al matrix surface what helped with their easier localization. On the other hand used preparation misrepresented proper view of seen dispersoid thickness.

The mechanical properties in tension were measured on specimens with the gauge of Ø3–30 mm using ZWICK testing machine at the strain rate of 0.03 and 3 min^{-1}. Extruded samples were tested longitudinally in respect to the extrusion direction. When tensile tests were performed at elevated temperatures samples were heated up for 20 min in order to reach desired testing temperature with 10 min dwell, at this temperature prior test was committed. Actual temperature at the tensile specimens was measured by thermocouple placed on the middle of specimen neck. Tensile specimens for creep tests had gauge dimensions of Ø6–20 mm.

3. Results and discussion

All consolidation routes yielded sound and dense (>99% THD) compacts. Fig. 1 shows SEM SE mode images of etched fine Al powder compacts obtained by means of direct extrusion – DE, forging – F and hot isostatic pressing – HIP. Fig. 2 shows respective BF TEM micrographs.

During DE powder particles experienced shearing resulting in their elongation into extrusion direction. No substructure within deformed grains was determined and each grain represents initial single powder particle. Enlargement of powder particle surface area during DE led to fracture of surface oxide skin into separate dispersoids. Dispersoids decorated grain boundaries of elongated particles (Fig. 2a). After DE some smaller Al powder particles remained undeformed, embedded among sheared grains. F with limited amount of induced shear led to isotropic microstructures of polyhedral grains (Figs. 1c and 2b). The microstructure consisted of Al single grains reinforced with continuous 3D oxide skeleton. Again each grain represents initial single powder particle. Microstructures after HIP recalled those obtained after F but native oxide layer fragmented and spheroidized into the large amount of small oxide dispersoids (about 100 nm in diameter) found along grain boundaries (Figs. 1d and 2c). Few residual plate-like oxide dispersoids are still seen. Identical microstructures to those found after HIP were obtained also after vacuum sintering of powder CIP performs at the minimal temperature of 520 °C, 12 h dwell time and 10^{-3} Pa vacuum pressure (Fig. 3a). Full density after vacuum sintering was conditioned by foregoing CIP state. Unlike unipressed samples, CIP accommodated sufficient fracture of oxide barrier as a key parameter for successful sintering to happen [15]. By means of EBSD mapping average grain sizes of 505 nm, 700 nm and 713 nm were calculated for DE (in transversal direction), F and HIP materials, respectively. It is apparent that spheroidized dispersoids stabilized the microstructures during HIP and vacuum sintering and no grain growth occurred. Selected area diffraction of oxide dispersion and 3D skeleton extracted from all types of samples revealed α-Al$_2$O$_3$ modification.

All materials showed superior thermal stability and retained their microstructures after 336 h annealing up to 450 °C. This was due to grain pinning effect of dispersoids (DE) and stability of 3D skeleton (F). First microstructural changes of DE and F materials were determined after severe exposure of compacts to 500 °C for 24 h. It led to spheroidization of oxide dispersoids of DE material (Fig. 3b) and fragmentation of 3D skeleton into spherical
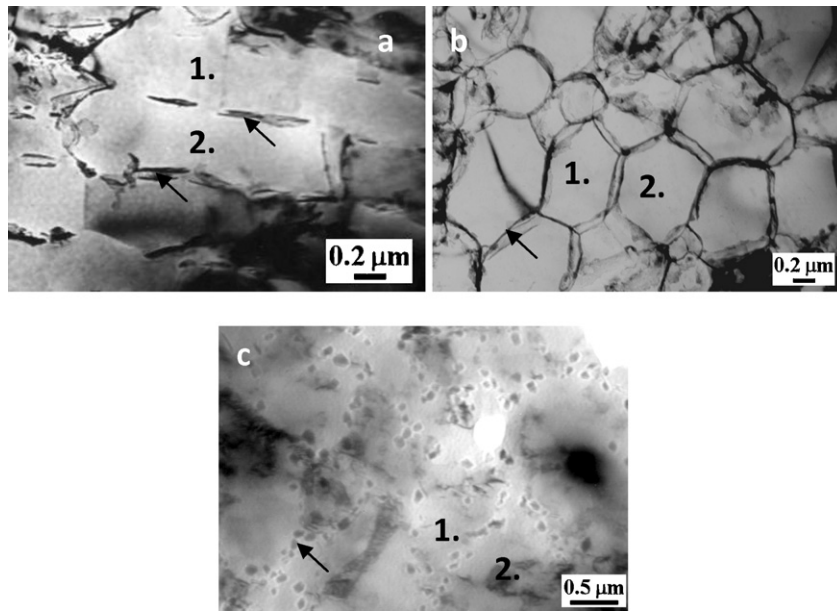
Fig. 2. BF TEM images of fine Al powder compacts produced via direct extrusion (a), forging (b), and HIP (c). Two adjacent Al grains are depicted with labels "1" and "2". The arrows indicate the alumina phase.
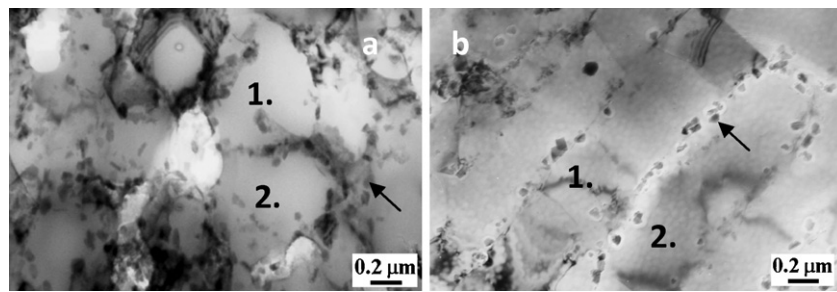

Fig. 3. BF TEM images of fine Al powder fully sintered after 12 h vacuum (10^{-3} Pa) sintering at 520 °C (a) and compact extruded at 450 °C after annealing at 500 °C for 24 h (b) [6]. Two adjacent Al grains are depicted with labels "1" and "2". The arrows indicate the alumina phase.

dispersoids in case of F material. Though, no apparent Al grain growth was determined. Microstructure of F material after annealing at 500 °C for 24 h was undistinguishable from as-HIPed material (Fig. 2c). Annealing treatments of HIP material up to 520 °C for 24 h accommodated no apparent microstructural changes.

Compact transport properties were found to be a good measure to evaluate the extent of the oxide fracture. As determined, electrical and thermal conductivities of as-cast Al (37.8 MS/m and 230 W/m K) were significantly reduced in case of F compacts with continuous oxide skeleton (5 MS/m and 65 W/m K). Fracture of oxide envelopes during compaction shifts conductivity towards the as-cast material, where 30.9 MS/m and 31.7 MS/m electrical conductivities were measured for DE and HIP compacts, respectively. (Fig. 4)

Table 1 summarizes ultimate strengths and ductility of powder compacts tested in tension at 20, 300 and 500 °C using strain rates of 0.03 and 3 min^{-1}. At room temperature DE compacts showed the highest strength. This was assured by grain boundary strengthening mechanism acting in the finest microstructures of DE compacts. Since the oxide dispersoids within DE and HIP compacts were predominantly found at the grain boundaries they cannot effectively contribute on strengthening by means of Orowan mechanism. At elevated temperatures stability of the grain interfaces becomes important [16]. Herein, Al + continuous Al$_2$O$_3$ skeleton composite structure of F material yielded smaller strength drop as the testing

temperature increased. UTS of 138 MPa of F material at 500 °C is far superior to any conventional Al alloy. Apparently, also fractured Al$_2$O$_3$ dispersoids contribute on stabilization of grain boundaries at
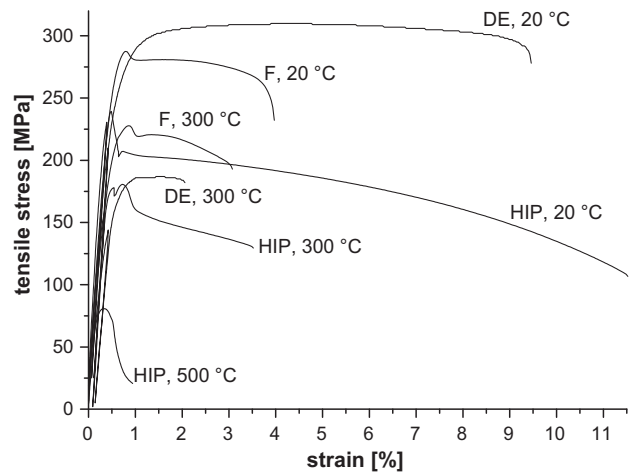

Fig. 4. Tensile tests of extruded, forged and HIPed Al powder compacts tested at 20, 300 and 500 °C (at strain rate 0.03 min^{-1}). Forged and extruded compacts fractured at 500 °C prematurely prior yielding.

Table 1
Ultimate strength (MPa)/ductility (%) of compacts obtained from tensile tests performed at 20, 300 and 500 °C using strain rates 0.03 and 3 min^{-1}.

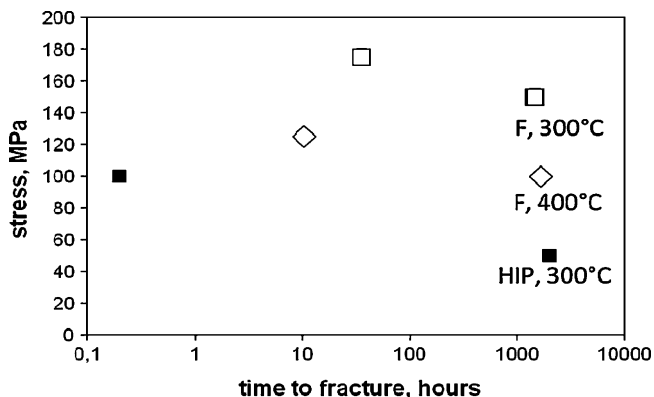| Testing temp. (°C)	0.03 min^{-1}			3 min^{-1}		
	Extruded	Forged	HIPed	Extruded	Forged	HIPed
20	310/9	287/3.5	230/11	302/7.5	293/6	223/7
300	186/2	227/3	180/3.5	206/10	–	175/4
500	70/0.5	138/0.5	81/1	120/2	153/1	97/2

Fig. 5. Time to fracture of forged (F) and HIP compacts subjected to creep tensile tests.

elevated temperatures but not in such large extent as continuous Al_2O_3 skeleton. This was supported by the improved creep performance of F compacts (Fig. 5). On the other hand, clean metal–metal grain boundaries of DE and HIP compacts yielded higher room temperature ductility. Significant decrease of the tensile ductility with increase of the testing temperature was consistent with other studies [16–18]. In these studies reduced fracture resistance at elevated temperatures was attributed speculatively to strain localization and plastic instability between growing microvoids. It was explained by dynamic recovery, which eliminates work hardening dislocation cell and source structures in submicron grains. That was consistent with found increase of ductility at elevated temperatures when higher strain rate of 3 min^{-1} was used (Table 1). Furthermore, it was proved by the presence of facet areas on fracture surfaces of DE samples tested at elevated temperatures shown earlier in [13]. Unlike DE compacts, F and HIPed compacts showed steep strength drop after reaching peak value, followed by flow softening (Fig. 4). This behaviour was avoided when strain rate increased to 3 min^{-1}. The reason for this behaviour remains unclear.

4. Conclusions

It was shown, that different powder metallurgy processing routes (extrusion, forging, and HIP/sintering) strongly affect the properties of subsequent fine ($d_{50} = 1.3 \mu m$) atomized Al 99.8% powder compacts. It was mainly due to the different distribution, morphology and interconnectivity of Al_2O_3 present on the surface of as-atomized powders after compaction. Extrusion and HIP disrupted native Al_2O_3 layer into separate nano-metric dispersoids found along compact grain boundaries. Forging yielded composite structures of polyhedral Al grains with a continuous interpenetrating Al_2O_3 skeleton. All compacts showed long-term thermal stability and enhanced mechanical properties up to 450 °C. On top of it, continuous Al_2O_3 skeleton within Al matrix led to superior mechanical properties and creep performance of forged compacts at elevated temperatures up to 400 °C. Furthermore, clean metal-metal grain boundaries assured higher room temperature ductility and conductivity of extruded and HIP compacts.

Acknowledgments

References

[1] R. Irman, Metallurgia 46 (1952) 125–133.
[2] R. Irman, Iron Age (1955) 104.
[3] Meyers Jr., O.D. Sherby, J. Inst. Met. 90 (1961–62) 380–382.
[4] A. van Zeerleder, Inst. Met. 75 (1948–49) 1143.
[5] C.L. Meyers Jr., J.C. Shyne, O.D. Sherby, Aust. Inst. Met. 8 (1963) 171.
[6] M. Balog, F. Simancik, O. Bajana, G. Requena, Mater. Sci. Eng. A 504 (2009) 1–7.
[7] X. Wu, W. Xu, K. Xia, Acta Mater. 57 (2009) 4321–4330.
[8] X. Phung, J. Groza, E.A. Stach, L.N. Williams, S.B. Ritchey, Mater. Eng. A 359 (2003) 261–268.
[9] B. Rufino, F. Boulc'h, M.-V. Coulet, G. Lacroix, R. Denoyel, Acta Mater. 55 (2007) 2815–2827.
[10] Y.C. Kang, S.L. Chan, Mater. Chem. Phys. 85 (2004) 438.
[11] C.L. Meyers Jr., K. Stulpe, Metallography 2 (1969) 41–56.
[12] New materials development G.m.b.H., http://www.nmd.at.
[13] M. Balog, J. Nagy, F. Simancik, K. Izdinsky, Int. J. Mater. Prod. Technol. 23 (2005) 69–78.
[14] M. Balog, M. Qian, G.J. Auchterlonie, G.B. Schaffer, In situ preparation of ultra fine grained Al–AlN composite – partial nitridation of fine aluminium powders (unpublished results).
[15] G.B. Schaffer, B.J. Hall, S.J. Bonner, S.H. Huo, T.B. Sercombe, Acta Mater. 54 (2006) 131–138.
[16] C. Poletti, M. Balog, F. Simancik, H.P. Degischer, Acta Mater. 58 (2010) 3781–3789.
[17] S.S. Kim, M.J. Haynes, R.P. Gangloff, Mater. Sci. Eng. A 203 (1995) 256–271.
[18] W.C. Port Jr., R.P. Gangloff, Metall. Trans. A 25 (1994) 365–379.